Molecular Basis of the Bohr Effect in Arthropod Hemocyanin*[s]

Shun Hirota[‡§1], **Takumi Kawahara**[§], **Mariano Beltramini**[¶], **Paolo Di Muro**[¶], **Richard S. Magliozzo**[||], **Jack Peisach**[**],
Linda S. Powers[‡‡], **Naoki Tanaka**[‡], **Satoshi Nagao**[‡], and **Luigi Bubacco**[¶2]

*From the ‡Graduate School of Materials Science, Nara Institute of Science and Technology, Nara, 630-0192 Japan, the
§Department of Physical Chemistry and 21st Century COE Program, Kyoto Pharmaceutical University, Kyoto, 607-8414 Japan,
the ¶Department of Biology, University of Padova, Padova, 35121 Italy, the ||Department of Chemistry, Brooklyn College, Brooklyn,
New York, 11210 the **Department of Physiology and Biophysics, Albert Einstein College of Medicine, Bronx, New York 10461,
and the ‡‡National Center for the Design of Molecular Function, University of Arizona, Tucson, Arizona 85721*

Flash photolysis and K-edge x-ray absorption spectroscopy (XAS) were used to investigate the functional and structural effects of pH on the oxygen affinity of three homologous arthropod hemocyanins (Hcs). Flash photolysis measurements showed that the well-characterized pH dependence of oxygen affinity (Bohr effect) is attributable to changes in the oxygen binding rate constant, k_{on}, rather than changes in k_{off}. In parallel, coordination geometry of copper in Hc was evaluated as a function of pH by XAS. It was found that the geometry of copper in the oxygenated protein is unchanged at all pH values investigated, while significant changes were observed for the deoxygenated protein as a function of pH. The interpretation of these changes was based on previously described correlations between spectral lineshape and coordination geometry obtained for model compounds of known structure (Blackburn, N. J., Strange, R. W., Reedijk, J., Volbeda, A., Farooq, A., Karlin, K. D., and Zubieta, J. (1989) *Inorg. Chem.*, 28, 1349–1357). A pH-dependent change in the geometry of cuprous copper in the active site of deoxyHc, from pseudotetrahedral toward trigonal was assigned from the observed intensity dependence of the $1s \rightarrow 4p_z$ transition in x-ray absorption near edge structure (XANES) spectra. The structural alteration correlated well with increase in oxygen affinity at alkaline pH determined in flash photolysis experiments. These results suggest that the oxygen binding rate in deoxyHc depends on the coordination geometry of Cu(I) and suggest a structural origin for the Bohr effect in arthropod Hcs.

Hemocyanins (Hcs)[3] are oxygen carrier and storage proteins found in molluscs and arthropods. Significant differences are observed between mollusc and arthropod Hcs in size of the functional units and in their tertiary and quaternary structures. Specifically, arthropod Hcs are structurally homogenous oligomeric proteins with a minimal functional subunit of 75 kDa. Under physiological conditions in the presence of calcium, the subunits are typically arranged in hexamers and dodecamers. Removal of Ca^{2+} with EDTA at neutral pH causes dissociation of the dodecamer into hexamers, which can be dissociated into monomers at alkaline pH (1). The different aggregation states are related to modified oxygen binding properties (2). As generally observed for respiratory proteins, a fundamental physiological property of Hc is its competence to bind oxygen with different affinity in response to allosteric effectors including hydrogen ions.

Detailed structural information concerning the active site of Hcs is derived mainly from a limited set of x-ray crystallographic investigations. The active site structures of the deoxy form have been described for two arthropod Hcs, *Panulirus interruptus* (3) and *Limulus polyphemus* (subunit II) (4). However, a comparison of the results is limited by the different solution conditions from which the proteins were crystallized. In both examples, each Cu(I) of the binuclear active site is coordinated by the ϵ-nitrogen of three histidine imidazole residues. In the *P. interruptus* structure obtained from protein crystallized at pH 4.8, two of the three histidine imidazole ligands and one copper atom lie nearly in a plane, with Cu-N bond lengths of 1.9 Å. In addition, each metal atom binds to a third histidyl imidazole nitrogen at a distance of 2.7 Å, perpendicular to the plane defined by the two equatorial histidine nitrogens and a copper atom. In contrast to this, the structure of *L. polyphemus* subunit II deoxyHc, obtained from crystals grown in 0.5 M chloride at pH 6.5–7.0, shows that each copper has approximately trigonal planar coordination geometry, with three histidyl imidazole nitrogens at a distance of 1.9–2.2 Å from the copper. These ligands define a plane from which the copper is displaced by 0.3 Å. An important additional difference between these two structures is the metal-metal distance, which is 3.6 Å in *P. interruptus* Hc (low pH and low ionic strength) and 4.6 Å for *L. polyphemus* Hc (physiological pH and higher ionic strength, Fig. 1).

The only example of an oxy structure for an arthropod Hc is that of subunit II of the *L. polyphemus* protein crystallized at pH 6.2 (5). In this example, the oxygen molecule is bound as a

charge transfer; SOD, superoxide dismutase; MES, 4-morpholineethanesulfonic acid.
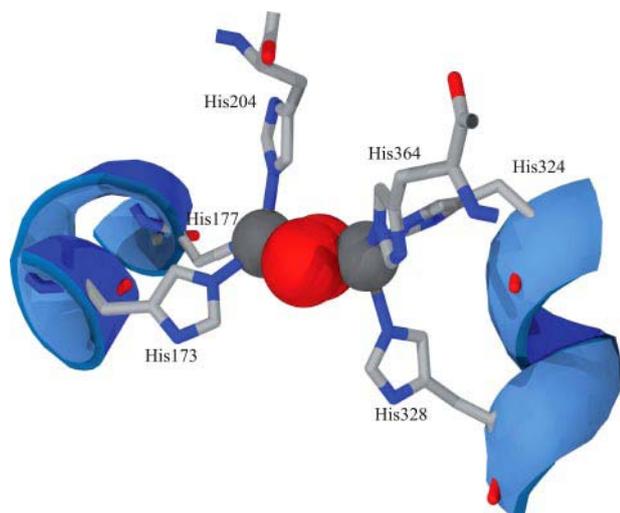
Bohr Effect in Hemocyanin

FIGURE 1. **oxyHc active site structure drawn from the x-ray crystal structure coordinates of *L. polyphemus* Hc (1OXY.pdb).** The software PDB-viewer (40) was used to illustrate the structures.

peroxide and forms a μ:η^2-η^2 bridge between the two Cu(II) atoms. Each copper atom is pentacoordinated in a square pyramidal geometry, where the equatorial plane is now defined by two histidyl imidazole nitrogens and the bound oxygen, while a third histidyl nitrogen is axially coordinated to copper. All three Cu-N bond lengths are 1.9 Å, and the metal-metal separation is 3.0–3.5 Å (6), a distance supported by EXAFS analysis for the closely related *P. interruptus* oxyHc (7, 8).

Oxygen binding to arthropods Hcs is very sensitive to pH, and the relevance of this Bohr effect resides in the capability of these proteins to respond to a pH variation in the medium with a variation in affinity for molecular oxygen to meet physiological needs. Although Hc has been studied extensively, detailed information concerning oxygen binding kinetics and the origins of both cooperativity and the Bohr effect are still limited (4–6). A useful approach for the study of oxygen binding kinetics is flash photolysis. OxyHc is blue and its optical spectrum is characterized by CT bands about 345 nm and at about 600 nm (9–12). DeoxyHc is colorless. Taking advantage of these optical differences, a photolysis approach was previously used to study the binding of oxygen to *Streptomyces antibioticus* tyrosinase, a monomeric enzyme that like Hc contains a binuclear copper center with similar optical properties (13).

In the present study, flash photolysis was used to investigate oxygen binding to Hc allowing us to probe allosteric effects. A complementary approach to the kinetic studies is x-ray absorption spectroscopy (XAS), which allows for the investigation of the immediate coordination geometry of Cu(I) in deoxyHc. For Cu(I), a species with limited potential for other spectroscopic studies as it lacks color and paramagnetism, coordination geometry can be deduced from copper k-edge absorbance measurements. Previous studies on Cu(I) model complexes of known structure provide the background information used to define a correlation between k-edge features and coordination geometry (14, 15).

Three paradigmatic arthropod Hcs that are structurally and functionally characterized were used here (2). Flash photolysis

was used to obtain the kinetic parameters of oxygen binding, while XAS was used to define structural features of copper centers in the active site as a function of pH. The results suggest that the O_2 binding rate depends on the coordination geometry of Cu(I) in deoxyHc providing evidence for a structural origin of the Bohr effect.

EXPERIMENTAL PROCEDURES

Sample Preparation—*P. interruptus* and *Carcinus aestuarii* Hcs were purified and stored as previously described (1, 16). *L. polyphemus* hemolymph was collected at the Marine Biological Laboratories, Woods Hole, MA. The clotted hemolymph was filtered through gauze and centrifuged to eliminate debris. The clear dark blue supernatant was dialyzed overnight at 4 °C against 20 mM $CaCl_2$, pH 7.0. During dialysis, a small amount of precipitate was formed and was separated by low speed centrifugation. The individual subunits were purified according to a published method (17). Subunit II was used in this study because of its well-characterized allosteric properties (18). The purity of the protein was verified by the electrophoretic mobility, while its aggregation state in the presence of Ca^{2+} was determined by analytical ultracentrifugation using Schlieren optics (18). Control oxygen binding experiments were carried out using a thin layer optical cell as previously described (19).

Flash Photolysis Measurements—Purified Hc of *C. aestuarii* in 50 mM Tris-HCl buffer, pH 8.3, was degassed on a vacuum line and then flushed with nitrogen gas. Hydroxylamine was added to the sample solution anaerobically (final concentration, 1 mM) to reduce any oxidized protein. The solution was then dialyzed under aerobic conditions against 50 mM Tris-HCl, MES, or acetate buffer at the desired pH. After dialysis, the protein concentration was adjusted to 20 μM, and a sample was placed under an atmosphere of oxygen plus nitrogen such that the partial pressure of oxygen could be varied from 5 to 100% with a mixed gas generator (MX-3S, Crown, Tokyo, Japan). The sample solution was filtered under the appropriate oxygen concentration and was transferred into the sealed quartz cell, which was filled with the same gas mixture.

Photolysis of oxyHc samples was accomplished using the third harmonic of an Nd:YAG laser (Surelight I-10, Continuum, Santa Clara, pulse energy, 30 mJ; pulse width, 5 ns) for excitation. Time-resolved absorbance changes were measured at 20 °C with illumination from a Xe lamp orthogonal to the laser pulse and were recorded on a digital oscilloscope (TDS 3012B, Tektronix, Tokyo, Japan), which received voltage signals from the photomultiplier attached to a monochromator (RSP-601-03, Unisoku, Osaka, Japan). The traces were obtained as the average of 256 or 512 pulses, and least-squares exponential fits were performed for the time-resolved absorption data using Igor Pro ver. 4.0 (WaveMetrics).

X-ray Edge Measurements—Highly concentrated Hc (2 mM copper concentration) used in spectroscopic experiments was prepared using a Centricon filter (Amicon) and then transferred to Lucite® sample holders designed for the x-ray measurements (20). DeoxyHc was obtained by passing a pre-humidified argon stream through an air tight, homemade chamber designed to host the loaded sample holders. Through the transparent faces (top and bottom) of the chamber, it was possible to

monitor the course of deoxygenation based on the disappearance of the blue color of oxyHc. It was estimated that no more than 2–3% oxyHc remained in the apparently colorless sample by visual inspection. After deoxygenation, the sealed chamber was cooled in liquid nitrogen and the frozen sample was removed and stored at 77 K until used. All samples were placed in a $25 \times 2.5 \times 2$ mm Lucite® sample holder covered with Kapton® tape.

X-ray fluorescence data were collected on beam lines X-9A and X-10C at the National Synchrotron Light Source (NSLS), Brookhaven National Laboratory, using double flat Si(111) (X-9A) and Si(220) (X-10C) crystal monochromators with fixed exit geometry. Beam harmonics were rejected using a nickel (X-9A) or rhodium- (X-10C) coated mirror positioned downstream of the monochromator. The sample temperature was maintained at ~120 K by flowing cooled nitrogen gas through a Lucite® cryostat as described previously (1). X-ray edge data having 3 eV resolution (X-9A) and 2 eV resolution (X-10C) were recorded by counting at single energy values for 3 s and incrementing the energy in 0.5 eV steps from 30 eV below the copper edge to 120 eV above the edge. Copper foil was used as an energy standard to account for any shifts in the monochromator calibration for any individual scan. Kapton® tape was mounted at a 45° angle to the incident x-ray beam to scatter x-ray photons through the copper foil. The photons were then counted with a photomultiplier tube positioned perpendicular to the x-ray beam as previously described (1). X-ray flux was 1.0×10^{10} (X-9A) and 1.3×10^{10} photons sec^{-1} mm^{-2} at 100 mA beam current (X-10C). X-ray edge data were generally taken in the range of 100–225 mA. K-copper fluorescence was detected with a 13-element solid-state energy-resolving germanium detector, and incident photon scattering was rejected by a nickel filter. Reference signals (incident beam intensity, I_o) were collected using a standard ion chamber. To monitor the condition of samples after x-ray exposure, optical spectra in the UV and visible regions were collected after sample dilution in buffer. Sample integrity was verified by the ratio between the absorbance at 280 nm and the charge transfer transition of oxyHc at 345 nm. No significant difference was found in this ratio collected before and after the XAS experiments.

X-ray edge spectra were normalized by fitting a function to pre- and post-edge regions of the spectrum and normalizing the edge jump to 1.0 at 9060 eV. To rule out systematic errors, partial sums of the total number of scans were independently fit without any significant differences noted.

RESULTS

Flash Photolysis of Oxygen from Oxyhemocyanin—The absorbance change after flash photolysis of *C. aestuarii* oxyHc was monitored at 337 nm, the absorption maximum of the oxyHc spectrum (Fig. 2). To prove that the observed optical change corresponded to oxygen photolysis and re-binding, the wavelength dependence of the initial absorbance change at several wavelengths within the absorption envelope of oxyHc was measured, and this action spectrum is depicted in the *inset* of Fig. 2. In the same figure, the difference absorption spectrum between oxyHc and deoxyHc is
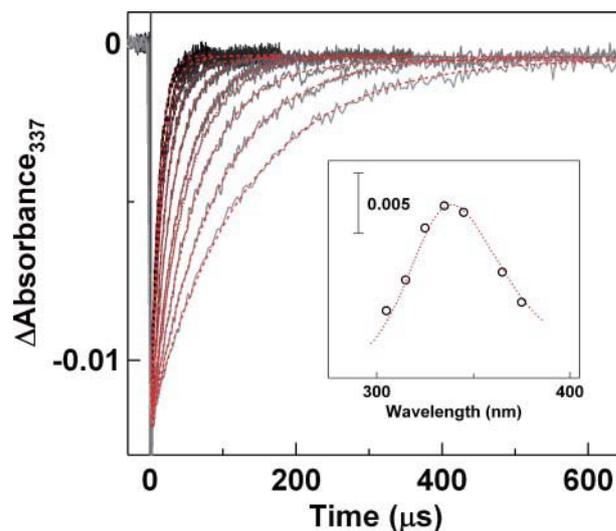

FIGURE 2. **Flash-photolysis measurements of *C. aestuarii* oxyHc.** Absorbance changes at 337 nm by 355-nm pulse irradiation under various oxygen concentrations are shown. Single exponential best-fitted curves are indicated by *red lines*. Experimental conditions: 20 μM Hc; 20 mM Ca^{2+}, 50 mM Tris-HCl buffer, pH 8.3; laser pulse, 30 mJ, 10 Hz; 20 °C; [O$_2$], 0.07, 0.14, 0.21, 0.28, 0.35, 0.49, 0.70, 0.91, 1.11, and 1.39 mM (remaining gas is N$_2$). Each trace is an average of 512 shots. *Inset*, wavelength dependence of the initial absorbance changes at the indicated wavelengths (*circles*) superimposed on the difference absorbance spectrum (*red line*, oxyHc minus deoxyHc).

shown (Fig. 2, *inset*, *dotted line*), which was well correlated with the wavelength dependence of the initial absorption change after photolysis. The experimental conditions were designed such that 100% of the Hc was in the oxygenated form before photolysis at all oxygen concentrations tested (1). The fraction of deoxyHc present at the beginning of detectable oxygen re-binding was about 5% calculated on the basis of the absorbance change. The time scale of absorbance recovery was in the range of microseconds to submilliseconds. The initial absorbance decrease corresponded to dissociation of oxygen from oxyHc, whereas the complete intensity recovery indicated re-binding of oxygen with no detectable photodamage.

The observed absorbance changes at 337 nm were fit successfully with single exponentials for all oxygen concentrations at pH 8.3. Although at this pH in the presence of Ca^{2+}, *C. aestuarii* Hc is known to be a mixture of 90% dimer of hexamers and 10% hexamers (1), there was no observable heterogeneity in the kinetic data. There was likewise no evidence for bi-phasic character that might be expected if the Hc were switching between the R- and T-state upon photolysis.

The observed oxygen re-binding rate constant (k_{obs}) increased upon increasing the pH from 6.5 to 8.7 (Fig. 3A). The k_{obs} values at pH 8.3 and 6.5 are plotted in Fig. 3B as a function of oxygen concentration; the dependence of k_{obs} on oxygen concentration was steeper for the measurements at pH 8.3 than that at pH 6.5. As will be discussed later, the ordinate intercept of the plots gave coincident k_{off} values, demonstrating that only the k_{on} values are pH-dependent. The shape of the optical spectrum of oxyHc is pH-independent, such that optical spectra at different pH values are superimposable. Therefore, our flash
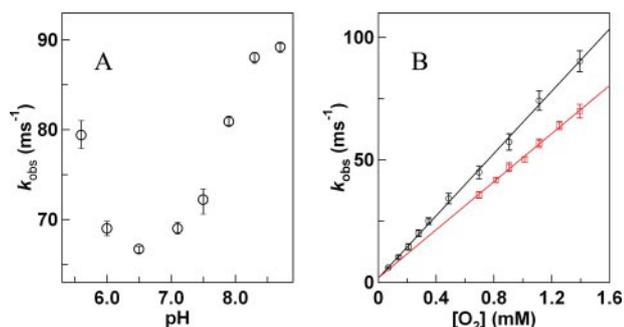
FIGURE 3. *A*, oxygen binding rate constants for *C. aestuarii* Hc at pH 5.6 to 8.7. Acetate, MES, and Tris-HCl buffers (50 mM), were used for measurements at pH 5.6, 6.0–6.5, and 7.1–8.7, respectively. *B*, plots of k_{obs} *versus* [O_2] for the reaction of Hc with oxygen at pH 8.3 (*black*) and 6.5 (*red*), together with the least-squares-fitted line according to Equation 1. Experimental conditions are the same as those listed in Fig. 2.

photolysis approach does not require any correction for pH effects on the spectrum of oxyHc.[4]

The absorbance change upon photolysis of oxyHc at pH 7.1 under O_2 concentrations lower than 0.35 mM could not be successfully fit with a single exponential curve (supplemental Fig. S1, depicts the case for [O_2] = 0.14 mM), although single exponential fits were adequate for Hc at pH 8.3 under all oxygen concentrations studied, and at pH 7.1 under higher oxygen concentrations ([O_2] > 0.49 mM). For the samples at pH 7.1 under oxygen concentrations less than 0.35 mM, double exponential curves were required to fit the data, suggesting a second process is operative under these conditions. The cooperative homohexamers of CaeSS3 subunits of Hc (1), exhibited only a single phase at pH 7.5 and [O_2] = 1.39 mM, with smaller k_{obs} values than the heterohexameric native protein (*Cae*SS3 homohexamers, 61 ± 5 ms^{-1}; the heterohexameric native protein 72.2 ± 3.2 ms^{-1}).

To calculate thermodynamic parameters for the oxygen rebinding reaction, we studied the temperature dependence of k_{obs}. In the tyrosinase case (13), the initial intensity change in absorbance in the photolysis experiments depended on temperature such that as the temperature increased, the intensity change increased, whereas for Hc, there was no observed temperature dependence of the optical features. These observations suggest that the structure of Hc at the active site is more rigid than that of tyrosinase (13) and that the increase in the oxygen-binding rate constant in Hc as a function of temperature is not due to protein structural changes. A linear Eyring plot was obtained based on the temperature dependence of k_{on} within the range 5 to 25 °C (Fig. 4). The activation enthalpy and entropy of oxygen binding to Hc calculated from the temperature dependence were as follows; $\Delta H^{\ddagger}$ = 7.2 kcal/mol and $\Delta S^{\ddagger}$ = −26 cal/(mol·K), respectively, based on the data in Fig. 4. These values compare reasonably well with those reported for oxygen binding to binuclear copper model complexes (21).

Copper K-edge Spectra of Arthropod Hemocyanin—Oxy and deoxyHc have readily distinguishable x-ray absorption spectra. For example, a comparison of the copper k-edge spectra of oxy
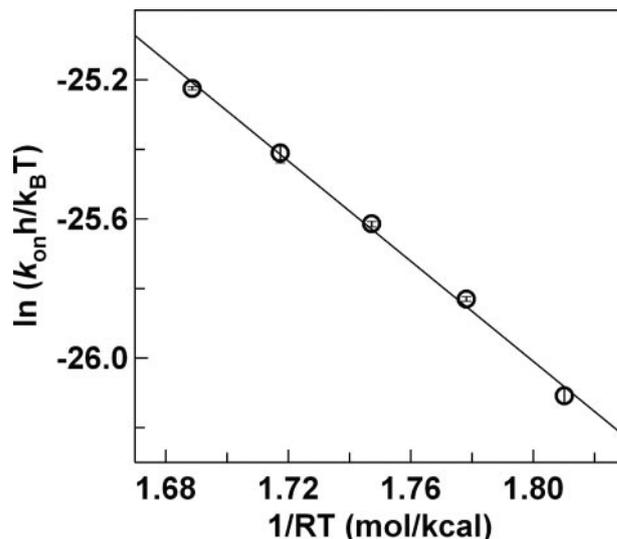
---

[4] The k_{obs} value also increased on the low pH side of the minimum at 6.5 (Fig. 3*A*) as has been noted before for an analogous arthropod Hc (23). This phenomenon is not analyzed further.

FIGURE 4. **Temperature dependence (5–25 °C) of oxygen binding rate constants for *C. aestuarii* Hc.** Experimental conditions are the same as those in Fig. 2, except Tris-HCl buffer, pH 7.8, was used. k_B is the Boltzmann constant.
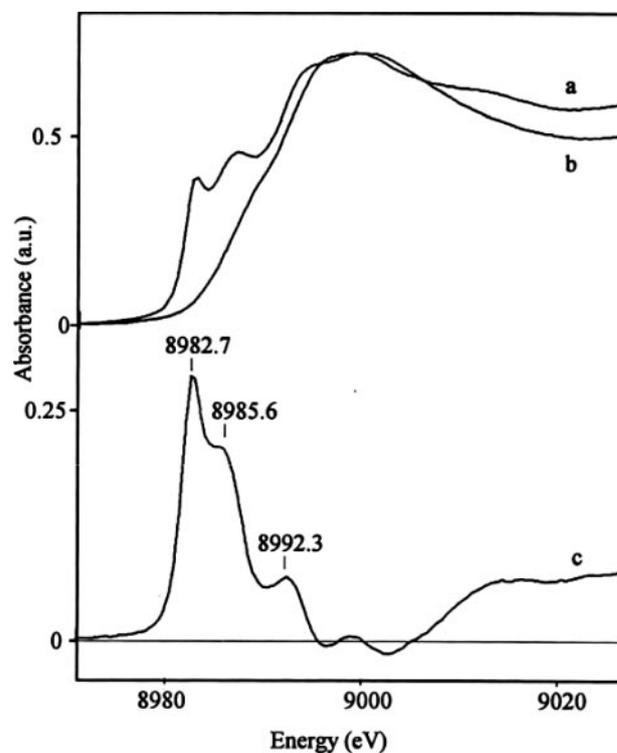

FIGURE 5. **K-edge x-ray absorption spectra of *P. interruptus* Hc.** *a*, DeoxyHc; *b*, oxyHc; and *c*, difference spectrum obtained by subtraction of the oxyHc spectrum from the deoxyHc spectrum. Both experimental spectra were collected from samples in 50 mM Tris-SO$_4$ buffer, pH 9, containing 20 mM CaCl$_2$.

and deoxy forms of *P. interruptus* Hc (Fig. 5), a very close homolog of *C. aestuarii* Hc, indicates a shift of 2–3 eV to higher energy expected from the increase in the 1s-electron binding energy for the metal ion in the oxy protein because of its cupric character (14). The difference spectrum between deoxy and oxyHc allows for an accurate determination of the peak positions in the edge spectra of the deoxy protein. The two largest absorbance difference peaks, at 8982.7 ± 0.5 and 8985.6 ± 0.5

TABLE 1
Values of P_{50} for oxygen binding to Hcs as a function of pH in the presence of 10 mM CaCl$_2$

	pH	P_{50} O$_2$ mmHg
P. interruptus	5.25	172[a]
	7	42[b]
	9	5[b]
C. aestuarii	7.1	44.3[c]
	7.5	33.7[c]
	7.9	13.6[c]
	8.3	6.81[c]
Subunit II *L. polyphemus*	7	2.5[d]
	9	1.4[d]

[a] In 100 mM Bis-Tris, pH 5.25 (30).
[b] In 50 mM Tris-HCl, pH 7 and in 50 mM ethanolamine, pH 9 (31).
[c] In 50 mM Tris-HCl (1).
[d] In 100 mM Tris-HCl, pH 7 and 9 (23).
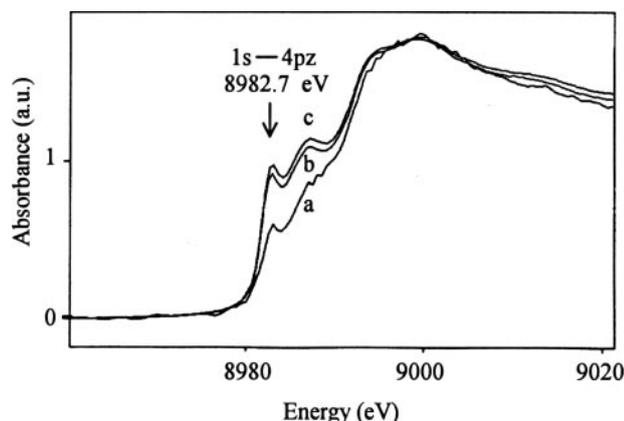
FIGURE 6. **K-edge x-ray absorption spectra of *P. interruptus* deoxyHc.** *a*, pH 5 in 50 mM acetate buffer; *b*, pH 7 in 50 mM Tris-SO$_4$ buffer; *c*, pH 9 in 50 mM Tris-SO$_4$ buffer. CaCl$_2$ (20 mM) was present in all samples.

FIGURE 7. **K-edge x-ray absorption spectra of subunit II of *L. polyphemus* deoxyHc.** *a*, pH 6 in 10 mM Tris-SO$_4$ buffer; *b*, pH 9 in 100 mM Tris-SO$_4$ buffer; *c*, pH 9 in 50 mM Tris-SO$_4$ buffer plus 500 mM NaCl; *d*, pH 6 in 50 mM Tris-SO$_4$ buffer plus 500 mM NaCl. CaCl$_2$ (20 mM) was present in all samples. The buffer concentrations for *a* and *b* were chosen to compensate for ionic strength effects.

eV, have been assigned to the $1s \rightarrow 4p_z$ and $1s \rightarrow (s+p)^*$ transitions, respectively (15). In a separate study, the intensities of these transitions were correlated with the coordination geometry of Cu(I) based on a systematic analysis of x-ray edge spectra for a collection of model complexes having different coordination geometries but the same tridentate nitrogen ligands (20, 22, 24). More precisely, the intensity of the 8982.7 eV feature, normalized to the edge jump, was found to be inversely proportional to the mean displacement along the *z*-axis of Cu(I) from the plane defined by the three directly coordinated nitrogen atoms. The intensity is significantly higher for the metal ion coordinated in a trigonal planar geometry compared with that for pseudotetrahedral geometry, in which the copper atom lies out of the plane defined by the ligands (20, 24). Therefore, the 8982.7 eV feature can serve as a spectroscopic probe of coordination geometry in Cu(I) sites with all nitrogen coordination as in deoxyHc and was used here to define the structural modifications induced by changes in pH.

The k-edge spectra for *P. interruptus* deoxyHc at different pH values are collected in Fig. 6. The oxygen affinity of this Hc increases ~35-fold from pH 5 to 9 (Table 1) (25, 26). At pH 5.25, the intensity of the 8982.7 eV feature is low (Fig. 6*a*). As the pH is raised to 7, and finally to 9, the intensity increases (Fig. 6, *b* and *c*). This spectroscopic change is indicative of the alteration of Cu(I) geometry from pseudotetrahedral toward trigonal (22). The spectral changes observed are not due to oxidation of Cu(I) to Cu(II) because the lineshape of the x-ray absorption edge

spectra collected at different pH values overlay in the 9000 eV region, with no indication of an energy shift expected if Cu(I) were oxidized to Cu(II). A smaller increase in the intensity of the 8982.7 eV feature with increasing pH was noted for subunit II of *L. polyphemus* Hc (Fig. 7) compared with the data described for *P. interruptus* Hc. This protein also has a Bohr effect (18), and the structural modulation induced by pH is considered here to be analogous to that described for *P. interruptus* Hc, indicating the general nature of the observations and also establishing a correlation between the magnitude of the Bohr effect and the observed intensity changes for two different Hcs. *C. aestuarii*, *P. interruptus*, and *L. polyphemus* Hcs are highly homologous and show the same trend in the pH dependence of oxygen binding.

DISCUSSION

Structural Features of Deoxyhemocyanin—In this study, the coordination geometry of copper in deoxyHc was investigated using x-ray spectroscopy. Data for the protein are interpreted based on k-edge absorption spectra for several Cu(I) model complexes of known structure, which show a correlation between the intensity of the 8982.7 eV ($1s \rightarrow 4p_z$) transition and geometry; high intensity corresponds to trigonal planar coordination (22, 27) and low intensity occurs for pseudotetrahedral symmetry (C_{3v}), because of mixing of s orbital character into the final state wave function (22). The observed increase in intensity of the $1s \rightarrow 4p_z$ transition with increasing pH values for both *P. interruptus* and subunit II of *L. polyphemus* deoxyHcs is interpreted as a change in coordination geometry from pseudotetrahedral at low pH toward trigonal planar at high pH. This change in structure is suggested to correlate with the Bohr effect known for the proteins investigated here. Pseudotetrahedral coordination geometry at low pH for Hc in solution is in agreement with the x-ray crystal structure of *P. interruptus* deoxyHc at pH 4.8 (3). The trigonal geometry of the high pH form of Hc cannot be corroborated by a comparison with an x-ray crystal structure as none is available at alkaline pH. It may be noted that the k-edge spectrum of Cu(I) in reduced SOD (28) closely resembles that of the high pH form of deoxyHc in terms

Bohr Effect in Hemocyanin

of the relative intensity of the 1s $\rightarrow$ 4p$_z$ band compared with the edge jump. The x-ray crystal structure of reduced SOD (Pdb file1dsw) shows a trigonal coordination geometry for Cu(I), with three nearly equal Cu-N bond lengths and angles of 120° between these bonds, similar to the crystal structure for Hc at high pH. It is suggested that for deoxyHc, the changes in geometry as a function of pH and the resulting changes in oxygen affinity derive from constraints on the active site in response to changes in protein conformation.

Modulation of Oxygen Affinity in Hemocyanin—The interplay of many factors enters into the mechanism of oxygen binding and the modulation of oxygen affinity in Hcs. These include the coordination geometry of the copper, accessibility of the active site, the Cu-Cu distance and the redox potential of the copper. The latter is important since oxygenation involves electron transfer from each Cu(I) to oxygen to yield a Cu(II)-O$_2$-Cu(II) structure. Allosteric effectors may influence oxygen binding by producing alterations in the tertiary and quaternary structure of the multimeric proteins and their subunits that have effects on the active site. Here, we have focused on copper (I) coordination geometry as a parameter not recognized before as one having an impact on Hc function.

The flash photolysis results provide a quantitative approach to analyze the relationship between k_{on} and oxygen affinity. The observed rate constant may be described according to Equation 1 (28).

$$k_{obs} = k_{on}([\text{deoxyHc}] + [\text{O}_2]) + k_{off} \quad \text{(Eq. 1)}$$

Because close to 100% of Hc was oxygenated in all samples (Hc concentration is 1 μM and dissolved O$_2$ is 220 μM or greater) and less than 5% of the total protein is monitored in the re-binding experiment, the deoxyHc concentration term can be neglected in Equation 1. Least squares fitting of a plot of k_{obs} against [O$_2$] at pH 8.3 (Fig. 3B, *black curve*) using Equation 1, gives k_{on} and k_{off} = (6.35 $\pm$ 0.05) $\times$ 10^7 M^{-1} s^{-1} and 1,800 $\pm$ 500 s^{-1}, respectively. From these values, the oxygen dissociation constant (K_D) was calculated as 28 $\pm$ 8 μM at pH 8.3. This K_D value was relatively close to that calculated (13 $\pm$ 1 μM) from the reported binding constant for *C. aestuarii* Hc obtained from equilibrium measurements (1). The only other available kinetic parameters are k_{on} and k_{off} of oxygen binding in *P. interruptus* Hc obtained by temperature-jump and stopped-flow measurements, respectively (29). Although the reported K_D value for *P. interruptus* Hc is smaller (2.0–9.1 μM), most likely because the measurements were carried out in the presence of 100 mM NaCl, which is known to act as a heterotropic effector increasing oxygen affinity (30). From the temperature-jump measurement, a k_{on} value was estimated to be ~3.2 $\times$ 10^7 M^{-1} s^{-1}, which is close to the value found here, but again was measured in the presence of 100 mM NaCl.

Here, the slope of the fitted curve (Fig. 3B, *red curve*) for oxygen rebinding rate was lower for the data at pH 6.5 than 8.3, with a calculated k_{on} = (4.91 $\pm$ 0.06) $\times$ 10^7 M^{-1} s^{-1} and k_{off} = 1,800 $\pm$ 700 s^{-1}. While the k_{off} value remains the same at the two pH values within experimental error, the k_{on} value decreases at low pH. The observed pH dependence of k_{on} may be correlated with geometric flexibility of Cu(I), which can rea-
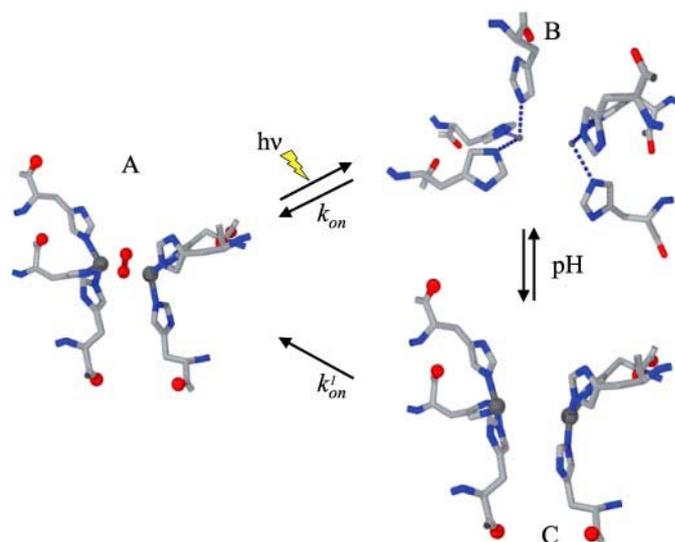

FIGURE 8. **Reaction scheme for oxygenation of arthropod hemocyanin including a change in geometry of copper in the deoxygenated active site with pH.** *A*, *Square pyramidal*, oxyHc active site structure drawn from the x-ray crystal structure coordinates of *L. polyphemus* Hc (1OXY.pdb); *B*, *trigonal*, active site of *P. interruptus* deoxyHc (1HCY.pdb) assumed here to be representative of the low pH form; *C*, *pseudotetrahedral*, active site of *L. polyphemus* deoxyHc (1LLA.pdb) assumed to closely represent the alkaline pH form. The software PDBviewer (40) was used to illustrate the structures. The k_{on} and k'_{on} represent the on-rates discussed in the text for the high and low pH conditions.

sonably be assumed to govern the modulation of oxygen affinity. The pH-independent character of k_{off} is consistent with the pH independence of both the optical spectra of oxyHc and the k-edge absorption properties of several oxyHcs (31). These observations are also consistent with the common square pyramidal structure for copper in the oxygenated Type III copper site found in tyrosinase (32), other Hcs (33) and catechol oxidase (34). Our results lead us to suggest that the Bohr effect for arthropod Hcs derives from structural modulation of the geometry of copper in deoxyHc rather than in oxyHc, according to the scheme presented in Fig. 8.

In the flash photolysis experiment, we are observing the behavior of a deoxygenated site in a nearly fully oxygenated R-state hexamer for the case at pH 8.3 and high oxygen concentration at pH 6.5. A plausible interpretation of the observed changes in k_{on} is that the single deoxygenated site that is part of R-state hexamers, may in the time frame of the experiment, rearrange into different structures (R') in response to the pH of the medium such that oxygen binding is favored at higher pH. Furthermore, oxygen binding data (1, 35) for both *C. aestuarii* and *Penaeus monodon* Hcs show that K_T and K_R both increase with pH (supplemental Fig. S2). The structural rearrangements of the deoxy site in the R multimer can then be the origin of the pH dependence of K_R, this parameter being the oxygen dissociation constant from the R state. Therefore, it seems reasonable, and it is the simpler interpretation, that the parallel pH dependences of K_T and K_R reported earlier arise from the same phenomenon, *i.e.* a change in the coordination geometry of Cu(I) in deoxygenated sites. This allows us to assume that the deoxy sites in the photolysis experiments are sensitive to pH in a similar way in a hexamer that is oxygenated or deoxygenated.

Central to this idea is the fact that all oxygenated type III structures reported from x-ray crystal data are superimposable, despite the fact that the Hcs are from organisms that belong to different *phyla*, and the proteins may have been crystallized at different pH values (3–4). Oxygen dissociation occurs from this unique structure, which would explain the pH independence of k_{off} values found here. It is reasonable then to suggest that a general mechanism for arthropod Hcs to modulate oxygen affinity involves a structural rearrangement in the deoxygenated protein that produces a change in k_{on}. This conclusion is substantiated by the comparison of Figs. 6 and 7 where a greater magnitude of spectral change was observed for *P. interruptus* deoxyHc compared with *L. polyphemus* Hc. The former protein has a greater difference in oxygen affinity per pH unit change than does *L. polyphemus* Hc. In further support of this concept, it should be noted that the presence of a Bohr effect for the binding of carbon monoxide to *P. interruptus* deoxyHc (36), a ligand that binds to only one copper, can be rationalized by a change in coordination geometry of a single Cu(I) with pH. Previous suggestions have focused instead on a change in copper-copper distance to explain the phenomenon (4, 6).

During oxygen coordination, ligand reorientations must occur as the copper coordination geometry is altered from distorted trigonal planar (or pseudotetrahedral) to square pyramidal in the Cu(II)-oxy form. A calculated reaction coordinate for reversible oxygen binding was investigated for Hc (24), and it was proposed that the protein matrix holds the Cu(I) ions in close proximity and therefore enables a simultaneous 2-electrons transfer. The structural effect of pH on the individual Cu(I) sites of the binuclear center proposed here may result in a modulation of both the redox potential of the individual copper ions and also the Cu-Cu distance.

The thermodynamic data reported here show that the $\Delta H^{\ddagger}$ and $\Delta S^{\ddagger}$ values for oxygenation of Hc are comparable to those reported for the $\mu:\eta^2-\eta^2$-peroxodicopper(II) and superoxo model compounds ($\Delta H^{\ddagger} = 8.9$ and 7.2 kcal/mol and $\Delta S^{\ddagger} = -15$ and -13 cal/(mol·K), respectively) (21). The similarity between the parameters for superoxo binding and peroxo binding and the overall similarities between the models and the results for Hc suggest that superoxo complex formation may be the rate-limiting step, and the peroxo species could be produced relatively easily from the superoxo species during the $\mu-\eta^2:\eta^2$-peroxodicopper(II) model complex formation and during Hc oxygenation as well. The latter is in agreement with a nearly simultaneous 2-electron transfer to O_2 as previously suggested (24). Also, the similarity in the parameters for Hc and the models suggests that despite the fact that the ligand must diffuse through the protein matrix to the active site, the interactions do not have an impact on the thermodynamics of oxygen binding.

It should be mentioned that the molecular basis of the Bohr effect proposed here implicates a structural change in coordination geometry for the copper only, leaving the question of identifying the role of individual amino acids to future studies. The ionization state of amino acids throughout the Hc molecule and changes in conformation of the polypeptide involved in the Bohr effect are expected to also affect the R/T equilibrium and the Hill coefficient, which combined produce the pH dependence of the oxygen binding parameters. Salt bridges between some conserved histidine and glutamate residues on the contact surface between monomers of *Eurypelma californicum* Hc (37) are proposed to be important. Possible mediators of allosteric signals have been recently described for *L. polyphemus* Hc (38). The deoxy protein is known to exhibit different conformations, which are evident in changes in the binding of small molecule allosteric effectors. Whether pH effects on the binding of these molecules and the Bohr effect are related remain to be demonstrated (39). However, unraveling the details of the mechanism that links the active sites in the oligomers leading to conformational changes, will require further study. In conclusion, the analysis presented here provides a reasonable general explanation of the structural relationship between metal geometry and the Bohr effect in arthropod Hcs.

REFERENCES

1. Dainese, E., Di Muro, P., Beltramini, M., Salvato, B., and Decker, H. (1998) *Eur. J. Biochem.* **256,** 350–358
2. Markl, J., and Decker, H. (1992) *Adv. Comp. Environ. Physiol.* **13,** 325–376
3. Volbeda, A., and Hol, W. G. (1989) *J. Mol. Biol.* **209,** 249–279
4. Hazes, B., Magnus, C., Bonaventura, C., Bonaventura, J., Dauter, Z., Kalk, K. H., and Hol, W. G. (1993) *Protein Science* **2,** 597–619
5. Magnus, K. A., Hazes, E. E., Lattman, A., Volbeda, A., and Hol, W. G. (1991) *Proteins: Struct. Funct. Gen.* **9,** 240–247
6. Magnus, K. A., Hazes, B., Ton-That, H., Bonaventura, C., Bonaventura, J., and Hol, W. G. (1994) *Proteins* **19,** 302–309
7. Feiters, M. C. (1990) *Comments Inorg. Chem.* **11,** 131–174
8. Volbeda, A., Feiters, M. C., Vincent, M. G., Bouwman, E., Dobson, B., Kalk, K. H., Reedijk, J., and Hol, W. G. (1989) *Eur. J. Biochem.* **181,** 669–673
9. Jolley, R. L., Jr., Evans, L. H., Makino, N., and Mason, H. S. (1974) *J. Biol. Chem.* **249,** 335–345
10. Heirwegh, K., Borginon, H., and Lontie, R. (1961) *Biochim. Biophys. Acta* **48,** 517–526
11. van Holde, K. E. (1967) *Biochemistry* **6,** 93–99
12. Solomon, E. I., and Lowery, M. D. (1993) *Science* **259,** 1575–1581
13. Hirota, S., Kawahara, T., Lonardi, E., de Waal, E., Funasaki, N., and Canters, G. W. (2005) *J. Am. Chem. Soc.* **127,** 17966–17967
14. Cramer, S. P., Eccles, T. K., Kutzler, F. W., Hodgson, K. O., and Mortenson, L. E. (1976) *J. Am. Chem. Soc.* **98,** 1287–1288
15. Smith, T. A., Penner-Hahn, J. E., Berding, M. A., Doniach, S., and Hodgson, K. O. (1985) *J. Am. Chem. Soc.* **107,** 5945–5955
16. Magliozzo, R. S., Bubacco, L., McCracken, J., Jiang, F., Beltramini, M., Salvato, B., and Peisach, J. (1995) *Biochemistry* **34,** 1513–1523
17. Brenowitz, M., Bonaventura, C., Bonaventura, J., and Gianazza, E. (1981) *Arch. Biochem. Biophys.* **210,** 748–761
18. Brenowitz, M., Bonaventura, C., and Bonaventura, J. (1984) *Arch. Biochem. Biophys.* **230,** 238–249
19. Kraus, D. W., and Wittemberg, J. B. (1990) *J. Biol. Chem.,* **265,** 16043–16053
20. Brown, J. M., Powers, L., Kincaid, B., Larrabee, J. A., and Spiro, T. G. (1980) *J. Am. Chem. Soc.* **102,** 4210–4216
21. Karlin, K. D., Tolman, W. B., Kaderli, S., and Zuberbühler, A. D. (1997) *J. Mol. Catal. A: Chemical* **117,** 215–222
22. Blackburn, N. J., Strange, R. W., Reedijk, J., Volbeda, A., Farooq, A., Karlin, K. D., and Zubieta, J. (1989) *Inorg. Chem.,* **28,** 1349–1357
23. Molon, A., Di Muro, P., Bubacco, L., Vasilyev, V., Salvato, Beltramini, M., Conze, W., Hellmann, N., and Decker, H. (2000) *Eur. J. Biochem.* **267,** 7046–7057
24. Metz, M., and Solomon, E. I. (2001) *J. Am. Chem. Soc.* **123,** 4938–4950
25. Kuiper, H. A., Coletta, M., Zolla, L., Chiancone, E., and Brunori, M. (1980) *Biochim. Biophys. Acta* **626,** 412–416
26. Kuiper, H. A., Gastra, W., Beintema, J. J., van Bruggen, E. F., Schepman,

A. M., and Drenth, J. (1975) *J. Mol. Biol.* **99,** 619–629

27. Kau, L. S., Spira-Solomon, D. J., Penner-Hahn, J. E., Hodgson, K. O., and Solomon, E. I. (1987) *J. Am. Chem. Soc.* **109,** 6433–6442

28. Blumberg, W. E., Eisenberg, P., Peisach, J., and Shulman, R. G. (1976) in *Iron and Copper Proteins* (Yasunobu, K. T., Mower, H. F., and Hayaishi, O., eds), pp. 389–399, Plenum, New York

29. Andrew, C. A., McKillop, K. P., and Sykes, A. G. (1993) *Biochim. Biophys. Acta* **1162,** 105–114

30. Brouwer, M., Bonaventura, C., and Bonaventura, J. (1978) *Biochemistry* **17,** 2148–2154

31. Sabatucci, A., Ascone, I., Bubacco, L., Beltramini, M., Di Muro, P., and Salvato, B. (2002) *J. Biol. Inorg. Chem.* **7,** 120–128

32. Matoba, Y., Kumagai, T., Yamamoto, A., Yoshitsu, H., and Sugiyama, M. (2006) *J. Biol. Chem.* **281,** 8981–8990

33. Cuff, M. E., Miller, K. I., van Holde, K. E., and Hendrickson, W. A. (1998)

J. Mol. Biol. **278,** 855–870

34. Klabunde, T., Eicken, C., Sacchettini, J. C., and Krebs, B. (1998) *Nat. Struct. Biol.* **5,** 1084–1090

35. Beltramini, M., Colangelo, N., Giomi, F., Bubacco, L., Di Muro, P., Hellmann, N., Jaenicke, E., and Decker, H. (2005) *FEBS J.* **272,** 2060–2075

36. Brunori, M., Zolla, L., Kuiper, H. A., and Finazzi Agrò, A. (1981) *J. Mol. Biol.* **153,** 1111–1123

37. Sterner, R., and Decker, H., (1994) *Proc. Natl. Acad. Sci. U. S. A.* **91,** 4835–4839

38. Martin, A. G., Depoix, F., Stohr, M., Meissner, U., Hagner-Holler, S., Hammouti, K., Burmester, T., Heyd, J., Wriggers, W., and Markl, J. (2007) *J. Mol. Biol.* **366,** 1332–1350

39. Menze, M. A., Hellmann, N., Decker, H., and Grieshaber, M. K., (2000) *Biochemistry* **39,** 10806–10811

40. Guex, N., and Peitsch, M. C. (1997) Electrophoresis **18,** 2714–2723